
Supplementary Materials for SmokeViz: A Large-Scale Satellite Dataset for Wildfire Smoke Detection and Segmentation

Anonymous Author(s)

Affiliation

Address

email

1 A Original Data and Software Licenses

- 2 The HMS smoke product does not have a license attached to it. For GOES imagery, NOAA states:
3 *"There are no restrictions on the use of this data"*. PyTroll is distributed under the GNU General
4 Public License v3.0, and Segmentation Models PyTorch is distributed under the MIT License.

5 B Satellite and Band Selection

- 6 As described in the main paper, Advanced Baseline Imager (ABI) bands 1-3 were selected for their
7 high signal-to-noise ratio (SNR) and relevance to visible smoke. Figure 10 shows an example of
8 GOES-West provides higher visibility of a smoke plume than GOES-East near sunrise. This effect is
9 consistent with Mie scattering physics, where forward-scattered light enhances contrast for aerosols
10 like smoke under favorable solar geometry.

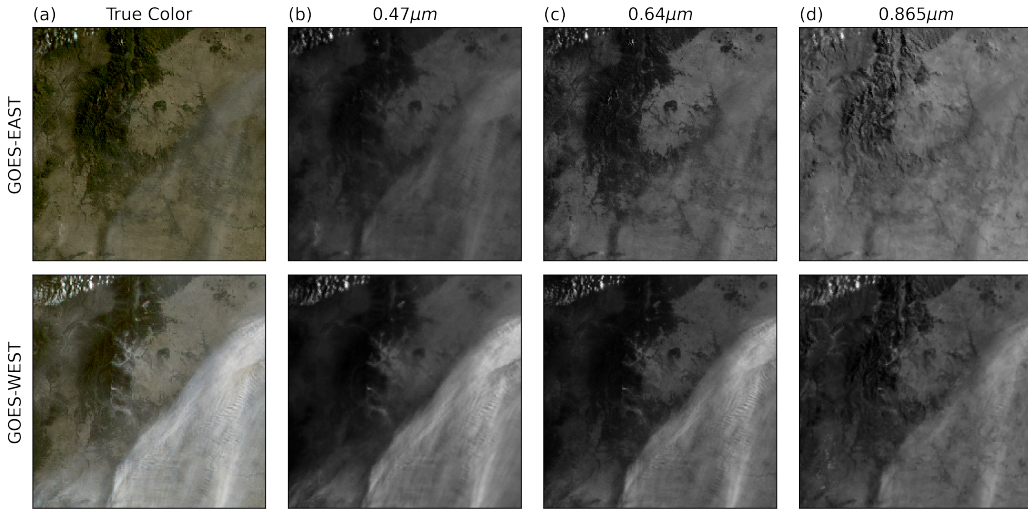


Figure 10: (a) True color GOES-EAST (top) and GOES-WEST (bottom) imagery from May 18th, 2022 centered at $(35.6^\circ, -105.0^\circ)$ in New Mexico, USA taken at 12:50 UTC. The GOES-East and West raw band imagery for (c) blue, (d) red and (e) veggie bands show variations in the SNR for smoke detection in relation to the λ of light being measured.

11 Figure 11 presents a smoke plume in a cloudy scene across all 16 ABI bands described in Table
 12 1. The smoke signal is prominent in Bands 1–3 but diminishes in subsequent NIR channels. Band
 13 C07 ($3.9\text{ }\mu\text{m}$), which is sensitive to thermal anomalies, shows a strong fire signal at the source of
 14 the plume. While useful for active fire detection, including C07 for smoke segmentation may bias
 15 models toward learning fire-smoke co-location, reducing generalization to detached or low opacity
 16 smoke plumes, especially those classified as light density that have traveled far from the source. This
 17 concern supports the decision to limit input channels in SmokeViz to those that reflect the analyst
 18 operational view while minimizing potential modeling shortcuts and dataset size. The SmokeViz
 19 dataset development code is designed to be easily adapted to incorporate any desired spectral bands
 20 and/or composites.

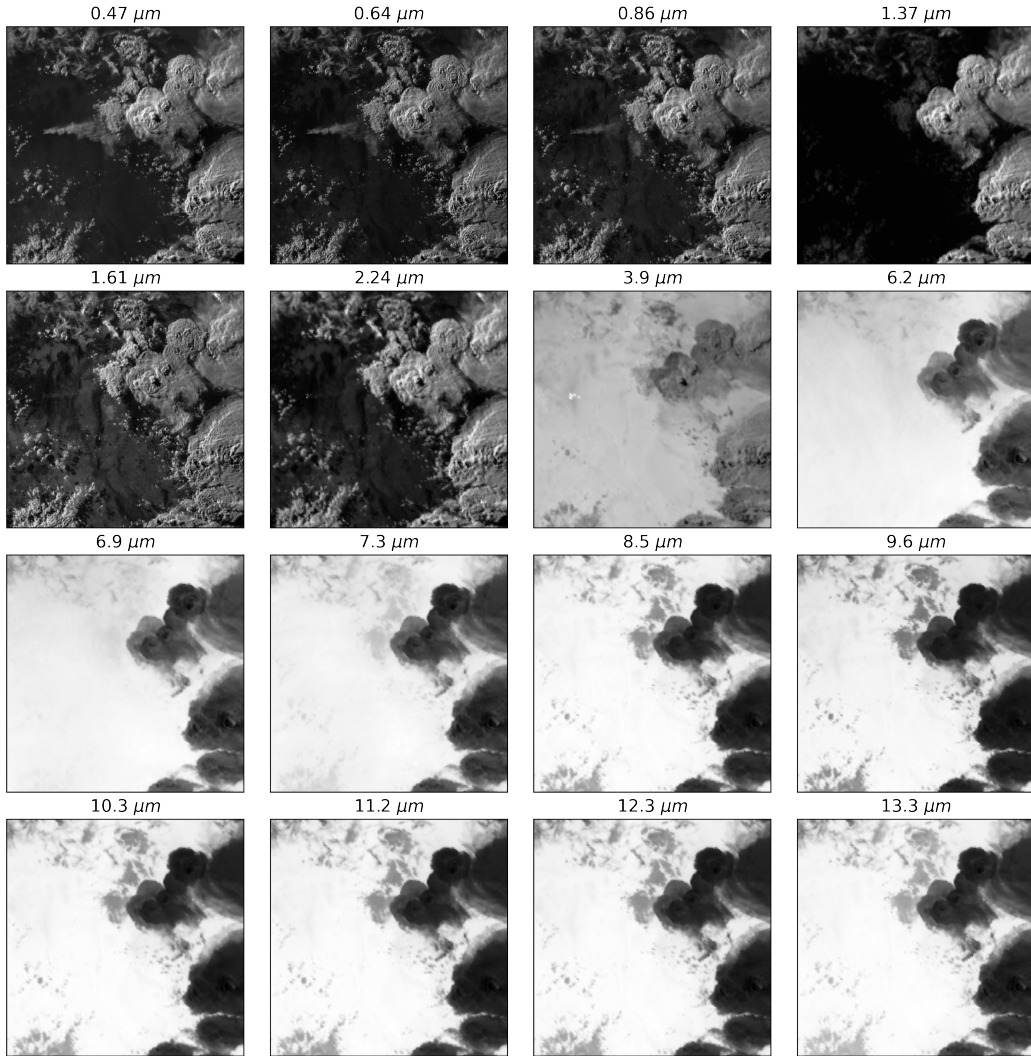


Figure 11: GOES-EAST imagery for all 16 bands from June 5th, 2022 centered at $(33.0^\circ, -106.0^\circ)$ in New Mexico, USA taken at 00:56 UTC.

21 **C Statistical Dataset Visualizations**

22 Figures 12–14 summarize key statistical characteristics of the SmokeViz dataset.

23 Figure 12 presents a histogram of the number of GOES satellite frames associated with each HMS
 24 annotation. Since frames are available every 10 minutes, this visualization reflects the variability in
 25 annotation time window duration. Most annotations span between 5 and 50 frames, corresponding

Table 1: The GOES-Series Advanced Baseline Imager (ABI) provides data at 16 channels that cover visible (C01-C02), near-IR (C03-C06) and IR (C07-C16) bands.

Band	Description	Center Wavelength (μm)	Spatial Resolution (km)
C01	Blue visible	0.47	1
C02	Red visible	0.64	0.5
C03	Veggie near IR	0.865	1
C04	Cirrus	1.378	2
C05	Snow/Ice	1.61	1
C06	Cloud particle	2.24	2
C07	Shortwave IR	3.9	2
C08	Upper-level water vapor	6.2	2
C09	Mid-level water vapor	6.9	2
C10	Lower-level water vapor	7.3	2
C11	IR cloud phase	8.5	2
C12	Ozone	9.6	2
C13	Clean longwave IR	10.35	2
C14	Longwave IR	11.2	2
C15	Dirty longwave IR	12.3	2
C16	CO_2	13.3	2

26 to 50 minutes to just over 8 hours, underscoring the need for resolving temporal ambiguity during
 27 dataset refinement.

28 Figure 13 shows the number of SmokeViz samples per year, stratified by smoke density. The year
 29 2020 exhibits the highest sample count, aligning with an exceptionally active wildfire season across
 30 North America [1]. The density distribution across years also varies, with some years showing a
 31 higher relative proportion of light or medium smoke annotations.

32 Lastly, SmokeViz includes annotations across North America, Figure 14 summarizes the dataset’s
 33 geographic coverage by country, including the United States, Canada, and Mexico.

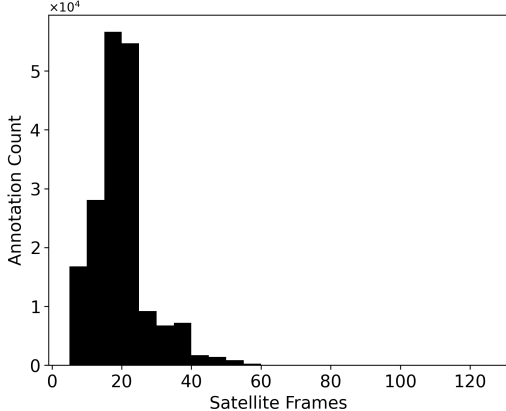


Figure 12: The number of annotations that span a number of satellite frames that are generated at a 10-minute interval.

34 D Agricultural Burns

35 The monthly peak in sample counts, shown in the main paper (Figure 6), occurs in March and April,
 36 preceding the typical wildfire season, which spans from late spring through fall. This early-season
 37 spike is likely due to prescribed agricultural burns, which are commonly conducted before vegetation
 38 exits winter dormancy [2]. Since HMS annotations do not distinguish between prescribed burns and
 39 wildfires, both event types are included in the dataset.

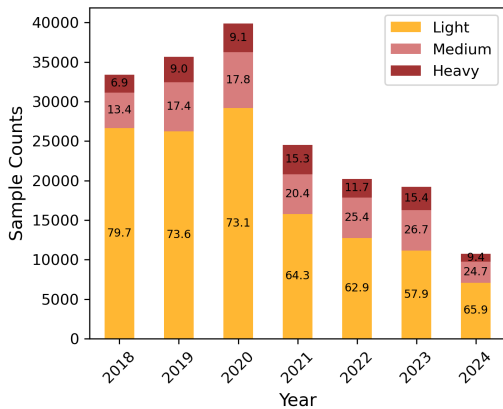


Figure 13: Annual sample counts in the SmokeViz dataset, broken down by smoke density class. Percentages within each column indicate the relative frequency of each density level for that year.

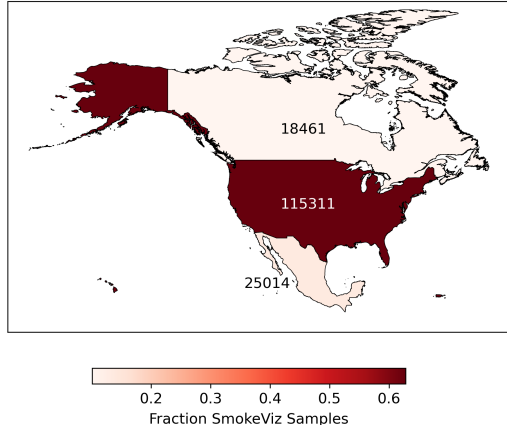


Figure 14: Proportion of samples in the SmokeViz dataset whose center pixel falls within Canada, the U.S.A., or Mexico. Sample counts are: Canada: 18,461; U.S.: 115,311; Mexico: 25,014. An additional 24,886 samples are centered over other countries or oceans.

- 40 Model performance over time, also shown in Figure 6, reveals that the highest IoU values for f_c on
 41 the \mathcal{D}_p test set occur during the peak wildfire season (May–September), not during the months with
 42 the highest sample counts. This suggests that prescribed burns that are typically smaller and less
 43 visually distinct than large wildfires, are more difficult for the model to segment.
 44 A spatial breakdown of sample density further supports this interpretation. Figure 7 in the main paper
 45 shows that the states with the highest number of samples are California, Georgia, and Florida. The ele-
 46 vated sample counts in southeastern states are consistent with regional practices of frequent prescribed
 47 burns. To investigate regional effects more explicitly, we divide the dataset into four geographic quad-
 48 rants—Northwest (NW), Southwest (SW), Northeast (NE), and Southeast (SE)—centered around a
 49 continental midpoint at ($40^{\circ}\text{N}, -105^{\circ}\text{W}$).
 50 Table 2 reports test IoU and sample counts for each quadrant. Despite containing the largest share of
 51 training samples, the Southeast quadrant exhibits the lowest model performance. This degradation
 52 is likely due to the abundance of prescribed burns, which may produce smaller, low-opacity smoke
 53 plumes that are harder to detect. For users whose objective is to train models specifically for large
 54 wildfire detection, this highlights a limitation of the dataset: a substantial portion of the training data
 55 originates from controlled burns, which may not be representative of the intended task. One possible
 56 mitigation strategy is to filter out short-duration annotations (e.g., single-day events), though this is
 57 complicated by variability in analyst-defined time windows and labeling cadence per fire event.

Table 2: SmokeViz dataset sample distribution and f_c test performance across geographic quadrants. Despite containing the most data, the Southeast (SE) region yields the lowest IoU.

Quadrant	SmokeViz Test Set IoU	SmokeViz Test Set Samples	SmokeViz Samples
Northwest (NW)	0.5887	4,177	32,792
Southwest (SW)	0.4590	1,937	34,267
Northeast (NE)	0.5822	1,133	13,342
Southeast (SE)	0.4798	12,977	103,271

58 E Satellite Analysis

- 59 Figure 15 shows the distribution of samples from GOES-East and GOES-West in both the full
 60 SmokeViz dataset and the \mathcal{D}_p test set, along with their respective segmentation performance using
 61 f_c . Although GOES-East contributes nearly three-quarters of all samples, model performance is

62 substantially better on GOES-West test samples, with an IoU of 0.6187 compared to 0.4498 for
63 GOES-East.

64 This discrepancy may stem from several factors. First, the observed signal quality varies between
65 satellites depending on diurnal lighting, seasonal solar angles, and atmospheric conditions. GOES-
66 West best captures forward-scattered sunlight during early morning hours over the western U.S.,
67 enhancing smoke visibility via Mie scattering and possibly boosting model accuracy. Additionally,
68 sensor calibration, viewing geometry, and line-of-sight differences between the two platforms could
69 contribute to systematic performance variation.

70 Another relevant factor is the operational transition between satellites. On June 18, 2022, GOES-17
71 was replaced by GOES-18 as the operational West satellite. While GOES-17 samples in the test set
72 yield an IoU of 0.6262, GOES-18 samples yield a slightly lower performance at 0.5852. This is likely
73 due to the limited exposure of GOES-18 data during model training: training years (2018–2021)
74 include only GOES-17, while GOES-18 is only present in the 2024 training data. This temporal
75 imbalance may partially explain the drop in IoU for GOES-18.

76 Overall, these results suggest that while GOES-East offers broader coverage, the more favorable
77 observational geometry of GOES-West—combined with consistent training data—produces stronger
78 segmentation results. Future work may explore satellite-specific fine-tuning or normalization tech-
79 niques to reduce these performance gaps.

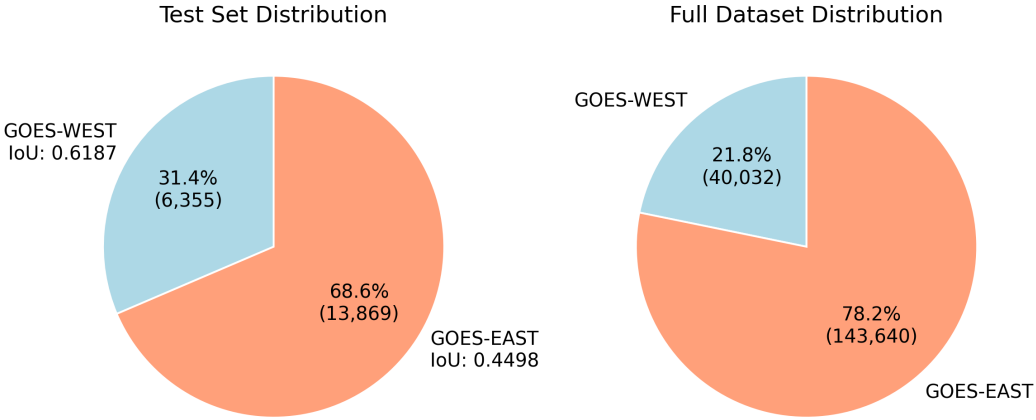


Figure 15: SmokeViz test set (left) and full dataset (right) sample distributions by satellite. GOES-West samples account for a smaller portion of the dataset but yield higher test IoU.

80 F Sunset/Sunrise Bias

81 As discussed in the main paper’s limitations, there exists a potential observational bias toward imagery
82 captured near sunrise or sunset. This bias may originate from both our Mie-derived dataset (\mathcal{D}_M) and
83 the original HMS annotations. Due to Mie scattering, the sun-satellite-smoke geometry results in a
84 higher signal-to-noise ratio (SNR) when the solar zenith angle is near 90°, typically around sunrise
85 and sunset. This light configuration enhances the visual detectability of smoke plumes, guiding our
86 initial selection method and potentially the analyst annotations.

87 In contrast, diurnal fire activity patterns . Wildfires tend to exhibit peak fire radiative power around
88 solar noon due to increased temperature and wind [3], meaning that smoke intensity and spread
89 are often greatest in midday imagery. The tension between observational clarity and fire behavior
90 complicates dataset curation.

91 Figure 16 compares the performance of models trained on \mathcal{D}_M (left) and the refined PLDR-generated
92 dataset \mathcal{D}_p (right), segmented by image with temporal proximity to sunrise/sunset versus midday. The
93 Mie-derived dataset favors high-SZA imagery, reflected in stronger IoU for morning/evening frames.
94 In contrast, the SmokeViz dataset (\mathcal{D}_p), which selects the frame with the best overlap between model

95 prediction and annotation, shows higher IoU for midday images, suggesting it more accurately aligns
96 with fire dynamics rather than SNR optimization bias.

97 This shift in temporal preference is further quantified in Figure 17, which shows the distribution of
98 frame differences between corresponding samples in \mathcal{D}_M and \mathcal{D}_p . Over 80% of the annotations were
99 assigned to different satellite frames between the two datasets. This illustrates the degree of temporal
100 refinement enabled by PLDR, which prioritizes semantic alignment over SNR.

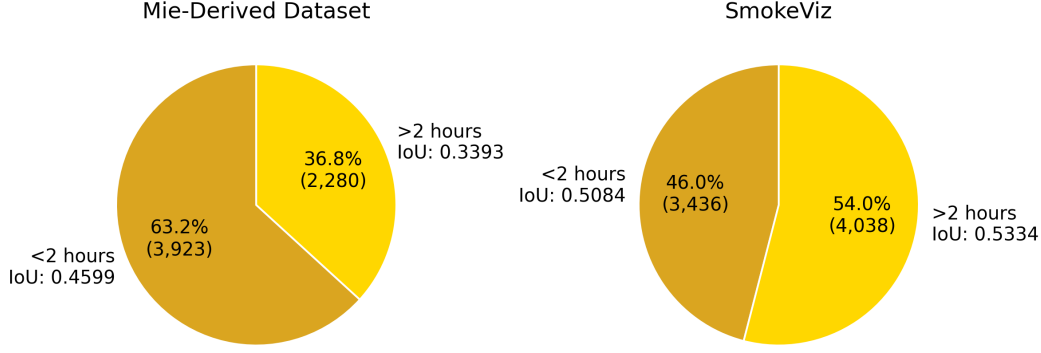


Figure 16: Distribution of test set samples in the Mie-derived dataset (\mathcal{D}_M , left) and SmokeViz dataset (\mathcal{D}_p , right), split by time proximity to sunrise/sunset versus midday. The PLDR refinement leads to large distribution and improved performance for midday samples.

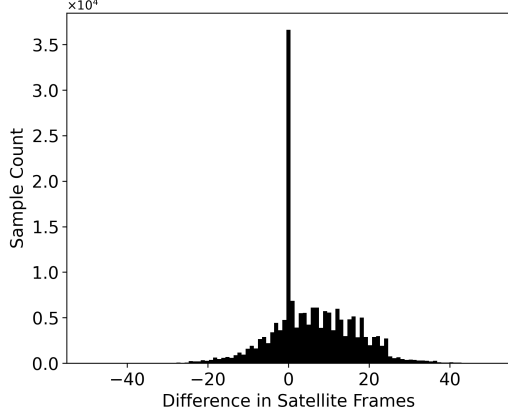


Figure 17: Histogram showing the shift in satellite frame selection between the Mie-derived dataset \mathcal{D}_M and the PLDR-selected SmokeViz dataset \mathcal{D}_p . A value of 0 indicates the same frame was selected. Only 20% of samples (36,608) used the same frame, indicating substantial temporal reassignment.

101 G Qualitative Analysis on Performance

102 Figure 18 gives some examples of when SmokeViz does not perform well in comparison to the HMS
103 analyst annotations. In the first column example, SmokeViz confuses a smoke-like cloud for smoke,
104 something it generally tends to not seem to have issues with, but this is an counter example to that
105 trend. The second through last columns all miss distinctive plumes that should be classified as either
106 medium or heavy density smoke. In contrast, we show what SmokeViz looks like when it performs
107 well in comparison to the HMS smoke product in figure 19.

108 To complement the quantitative evaluation, we provide qualitative comparisons between the SmokeViz
109 model predictions and the original HMS analyst annotations. These examples illustrate strengths and
110 failure modes observed in the dataset.

111 Figure 18 presents five cases where f_c does not perform optimally. In the first column, the model
 112 mistakenly identifies a smoke-like cloud as light-density smoke, a rare misclassification that reveals
 113 a potential weakness in cloud/smoke differentiation under certain lighting and texture conditions.
 114 In the remaining columns, SmokeViz underestimates the extent or density of visible smoke plumes.
 115 These errors generally occur in scenes with faint or fragmented plumes, where the signal-to-noise
 116 ratio is lower, or where overlapping atmospheric conditions make segmentation more difficult. In
 117 some cases, partial occlusion or lower contrast in the plume edges may have limited the model's
 118 confidence.

119 In contrast, Figure 19 shows examples where SmokeViz closely matches the HMS labels or even
 120 outperforms them in delineating plume boundaries. In these scenes, the model produces tighter
 121 boundaries that conform well to the visible smoke extent, including fine structural details that the
 122 coarser analyst polygons often miss.

123 Together, these examples show that while the model performs robustly across many diverse smoke
 124 scenes, it still faces challenges in edge cases involving ambiguous cloud formations, light plumes, or
 125 visually occluded conditions. These qualitative insights can help inform aspects of improvements in
 126 future models.

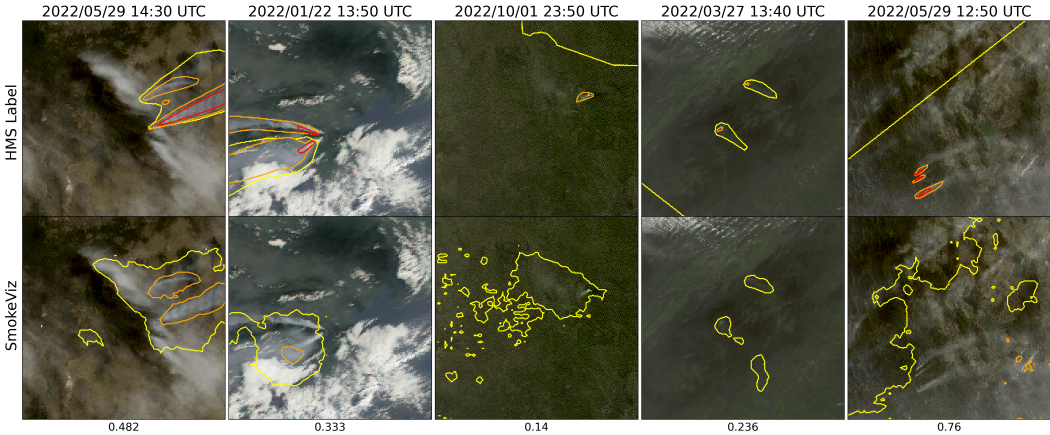


Figure 18: Challenging examples where SmokeViz underperforms. Top row: HMS annotations. Bottom row: SmokeViz model predictions. Leftmost column shows a false positive (cloud misclassified as smoke), remaining examples show under-segmentation or missed detection of smoke plumes. IoU values for each column are shown below.

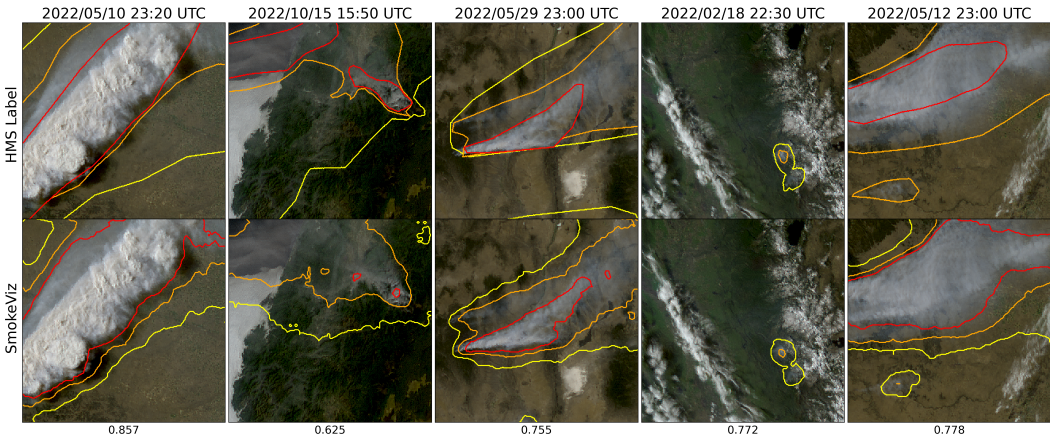


Figure 19: Examples of successful segmentation by SmokeViz. The model predictions (bottom) align well with HMS annotations (top), capturing plume shape and density more precisely. IoU scores shown below each sample indicate high overlap.

127 **H Machine Learning Reproducibility**

128 All relevant code for dataset construction, model training, and evaluation is publicly available
129 at <https://github.com/anonymous-smokeviz/SmokeViz> to ensure transparency and repro-
130 ducibility.

131 The models presented in this study are not optimized for state-of-the-art performance but are designed
132 to serve two primary purposes: (1) generate pseudo-labels used in the PLDR workflow to construct
133 the SmokeViz dataset, and (2) evaluate the relative performance of models trained on the Mie-derived
134 dataset (\mathcal{D}_M) versus the refined SmokeViz dataset (\mathcal{D}_p).

135 To select the parent model f_o , we trained several encoder-decoder architectures on \mathcal{D}_M and selected
136 the one that achieved the highest overall Intersection over Union (IoU), as shown in Table 3. The top-
137 performing model used EfficientNetV2 as the encoder and PSPNet as the decoder. This architecture
138 was then used to generate intermediary pseudo-labels for the PLDR process.

Table 3: Comparison of segmentation model IoU metrics on the Mie-derived dataset (\mathcal{D}_M). The highest overall IoU model (EfficientNetV2 + PSPNet) was selected as f_o .

encoder decoder	EfficientNet[4] PSPNet[7]	[4] DeepLabV3+[8]	EfficientViT[5] Segformer[9]	[5] UperNet [10]	ViT [6] DPT[11]
Heavy	0.3221	0.2893	0.2185	0.3099	0.2466
Medium	0.4288	0.4091	0.3977	0.4041	0.3135
Light	0.5044	0.4424	0.4331	0.4274	0.4964
Overall	0.4677	0.4172	0.4054	0.4098	0.4331

139 All models were trained using the Adam optimizer with a learning rate of 1×10^{-4} , batch size of
140 16, and 100 training epochs. Hyperparameter values were chosen based on memory constraints and
141 general suitability for large-scale semantic segmentation tasks.

142 **H.1 Datasheet for SmokeViz**

143 Questions from the <https://arxiv.org/abs/1803.09010> paper, v7.

144 **H.1.1 Motivation**

145 The questions in this section are primarily intended to encourage dataset creators to clearly articulate
146 their reasons for creating the dataset and to promote transparency about funding interests.

147 **For what purpose was the dataset created?**

148 SmokeViz was created to serve as a large labeled dataset to be used in creating wildfire smoke plume
149 related machine learning models. Applications include wildfire smoke detection or smoke dispersion
150 modeling.

151 **Who created the dataset (e.g., which team, research group) and on behalf of which entity (e.g.,
152 company, institution, organization)?**

153 REMOVED TO KEEP ANONYMITY DURING REVIEW PROCESS.

154 **Who funded the creation of the dataset?**

155 REMOVED TO KEEP ANONYMITY DURING REVIEW PROCESS.

156 **Any other comments?**

157 None.

158 **H.1.2 Composition**

159 Most of these questions are intended to provide dataset consumers with the information they need to
160 make informed decisions about using the dataset for specific tasks. The answers to some of these
161 questions reveal information about compliance with the EU's General Data Protection Regulation
162 (GDPR) or comparable regulations in other jurisdictions.

163 **What do the instances that comprise the dataset represent (e.g., documents, photos, people,
164 countries)?**

165 Each instance is a 256x256x3 RGB image from GOES imagery with an accompanying 256x256x3
166 binary masks corresponding to density of smoke. There are 3 densities of smoke - Light, Medium
167 and Heavy.

168 **How many instances are there in total (of each type, if appropriate)?**

169 There are 183,672 samples - 128,755 for light, 35,710 for medium and 19,207 for heavy density
170 smoke.

171 **Does the dataset contain all possible instances or is it a sample (not necessarily random) of
172 instances from a larger set?**

173 The entire possible number of samples between 2018/01/01 - 2024/11/01 is 210,702. The dataset is
174 reduced to 207,106 samples after filtering out any samples with no corresponding satellite imagery
175 available or imagery that is less than 10 or over 90 percent saturation. Total saturation is defined
176 when each pixel is equal to 1. Mentioned in more detail in the paper, the dataset was further reduced
177 down to 183,672 samples after applying a .01 IoU threshold during the pseudo-labeling process.

178 **What data does each instance consist of?**

179 The data is processed to correct for Rayleigh scattering, solar zenith angle and projected so each pixel
180 is representative of the same area of land. The algorithm is referenced in the SmokeViz paper.

181 **Is there a label or target associated with each instance?**

182 Yes, there are no samples that are intended to not display any smoke.

183 **Is any information missing from individual instances?**

184 We have seen imagery where smoke is labeled but there's adjacent smoke plumes that were unlabeled.
185 With human labels comes human errors.

186 **Are relationships between individual instances made explicit (e.g., users' movie ratings, social
187 network links)?**

188 Some instances can overlap in geographic location, there can be multiple smoke plumes in one
189 instance, but the index of the HMS smoke annotation is listed and can be mapped back to the original
190 dataset for geolocation information.

191 **Are there recommended data splits (e.g., training, development/validation, testing)?**

192 We recommend using full years of data for training, validation and testing to keep full year long
193 patterns of wildfire behavior. We use 2018-2021 and 2024 for training, 2023 for validation and 2022
194 for testing.

195 **Are there any errors, sources of noise, or redundancies in the dataset?**

196 The HMS smoke annotations that are used as truth are a source of noise as explained in the SmokeViz
197 paper. These include approximations of smoke polygons mismatching actual location and time
198 windows being too large that smoke moves during the time window. There is also noise caused by
199 atmospheric interactions with light. Redundancies occur when there more than one smoke plume and
200 annotation in one image.

201 **Is the dataset self-contained, or does it link to or otherwise rely on external resources (e.g.,
202 websites, tweets, other datasets)?**

203 The dataset is self-contained.

204 **Does the dataset contain data that might be considered confidential (e.g., data that is pro-
205 tected by legal privilege or by doctor-patient confidentiality, data that includes the content of
206 individuals' non-public communications)?**

207 No.

208 **Does the dataset contain data that, if viewed directly, might be offensive, insulting, threatening,
209 or might otherwise cause anxiety?**

210 No.

211 **Does the dataset relate to people?**

212 No, not directly, although wildfires do affect people, these images are at 1km resolution and do not
213 show enough detail to relate to people or infrastructure.

214 **Does the dataset identify any subpopulations (e.g., by age, gender)?**

215 No.

216 **Is it possible to identify individuals (i.e., one or more natural persons), either directly or
217 indirectly (i.e., in combination with other data) from the dataset?**

218 No.

219 **Does the dataset contain data that might be considered sensitive in any way (e.g., data that
220 reveals racial or ethnic origins, sexual orientations, religious beliefs, political opinions or
221 union memberships, or locations; financial or health data; biometric or genetic data; forms of
222 government identification, such as social security numbers; criminal history)?**

223 No.

224 **Any other comments?**

225 No.

226 **H.1.3 Collection process**

227 The answers to questions here may provide information that allow others to reconstruct the dataset
228 without access to it.

229 **How was the data associated with each instance acquired?**

230 The labels from HMS smoke product are not validated or verified but is used for AirNow air quality
231 assessments. The GOES imagery is collected by the ABI sensor and is corrected for any anomalies
232 and also converted from photon count to radiance values.

233 **What mechanisms or procedures were used to collect the data (e.g., hardware apparatus or**
234 **sensor, manual human curation, software program, software API)?**

235 Original low temporal resolution annotations were manual human analyst curated. To create the high
236 temporal resolution annotations, we use pseudo-labeling discussed in detail within the SmokeViz
237 paper.

238 **If the dataset is a sample from a larger set, what was the sampling strategy (e.g., deterministic,**
239 **probabilistic with specific sampling probabilities)?**

240 The HMS smoke analysts are only looking for smoke during the daytime and do avoid annotations
241 during heavy cloud cover.

242 **Who was involved in the data collection process (e.g., students, crowdworkers, contractors) and**
243 **how were they compensated (e.g., how much were crowdworkers paid)?**

244 The NOAA NESDIS employed analysts are compensated as salaried federal employees.

245 **Over what timeframe was the data collected?**

246 2018-2024

247 **Were any ethical review processes conducted (e.g., by an institutional review board)?**

248 No.

249 **H.1.4 Preprocessing/cleaning/labeling**

250 The questions in this section are intended to provide dataset consumers with the information they
251 need to determine whether the “raw” data has been processed in ways that are compatible with their
252 chosen tasks. For example, text that has been converted into a “bag-of-words” is not suitable for tasks
253 involving word order.

254 **Was any preprocessing/cleaning/labeling of the data done (e.g., discretization or bucketing,**
255 **tokenization, part-of-speech tagging, SIFT feature extraction, removal of instances, processing**
256 **of missing values)?**

257 The data was processed according to the GOES True Color paper referenced in the SmokeViz paper
258 methods section. This includes atmospheric, Rayleigh corrections and estimation of a Green band.

259 **Was the “raw” data saved in addition to the preprocessed/cleaned/labeled data (e.g., to support**
260 **unanticipated future uses)?**

261 The raw data is available from the NOAA AWS webpage. <https://registry.opendata.aws/noaa-goes/> The HMS smoke annotations are available here: <https://www.ospo.noaa.gov/products/land/hms.html>

264 **Is the software used to preprocess/clean/label the instances available?**

265 Yes, Pytroll implements the algorithm discussed in the GOES True Color paper referenced in the
266 SmokeViz paper.

267 **Any other comments?** None.

268 **H.1.5 Uses**

269 These questions are intended to encourage dataset creators to reflect on the tasks for which the dataset
270 should and should not be used. By explicitly highlighting these tasks, dataset creators can help dataset
271 consumers to make informed decisions, thereby avoiding potential risks or harms.

272 **Has the dataset been used for any tasks already?**

273 It was used to train benchmark models mentioned in the paper that apply semantic segmentation to
274 identify and classify smoke in satellite imagery.

275 **Is there a repository that links to any or all papers or systems that use the dataset?**

276 No.

277 **What (other) tasks could the dataset be used for?**

278 A machine learning based smoke dispersion forecast model, automated wildfire smoke detection and
279 segementation, a smoke analysis product for data assimilation into smoke or air quality models.

280 **Is there anything about the composition of the dataset or the way it was collected and prepro-
281 cessed/cleaned/labeled that might impact future uses?** No.

282 **Are there tasks for which the dataset should not be used?** No.

283 **Any other comments?** None

284 **H.1.6 Distribution**

285 **Will the dataset be distributed to third parties outside of the entity (e.g., company, institution,
286 organization) on behalf of which the dataset was created?**

287 No.

288 **How will the dataset will be distributed (e.g., tarball on website, API, GitHub)?**

289 <https://noaa-gsl-experimental-pds.s3.amazonaws.com/index.html#SmokeViz/>

290 **When will the dataset be distributed?**

291 It is currently available.

292 **Will the dataset be distributed under a copyright or other intellectual property (IP) license,
293 and/or under applicable terms of use (ToU)?**

294 No.

295 **Have any third parties imposed IP-based or other restrictions on the data associated with the
296 instances?**

297 No.

298 **Do any export controls or other regulatory restrictions apply to the dataset or to individual
299 instances?**

300 No.

301 **Any other comments?**

302 None.

303 **H.1.7 Maintenance**

304 These questions are intended to encourage dataset creators to plan for dataset maintenance and
305 communicate this plan with dataset consumers.

306 **Who is supporting/hosting/maintaining the dataset?**

307 National Oceanic and Atmospheric Administration Global Systems Laboratory is hosting the dataset
308 on Amazon Web Services.

309 **How can the owner/curator/manager of the dataset be contacted (e.g., email address)?**

310 REMOVED TO KEEP ANONYMITY DURING REVIEW PROCESS.

311 **Is there an erratum?**

312 No.

313 **Will the dataset be updated (e.g., to correct labeling errors, add new instances, delete instances)?**

314 Yes, only to add new instances.

315 **If the dataset relates to people, are there applicable limits on the retention of the data associated
316 with the instances (e.g., were individuals in question told that their data would be retained for a
317 fixed period of time and then deleted)?**

318 Not applicable.

319 **Will older versions of the dataset continue to be supported/hosted/maintained?**

320 No, it is too large to keep multiple versions.

321 **If others want to extend/augment/build on/contribute to the dataset, is there a mechanism for
322 them to do so?**

323 The code to extend/augment/build is publicly available [https://github.com/](https://github.com/anonymous-smokeviz/SmokeViz)
324 anonymous-smokeviz/SmokeViz. We encourage anyone that would like to contribute to
325 SmokeViz to reach out to REMOVED TO KEEP ANONYMITY DURING REVIEW PROCESS.

326 **Any other comments?**

327 None

328 **References**

- 329 [1] Jon E Keeley and Alexandra D Syphard. Large california wildfires: 2020 fires in historical
330 context. *Fire Ecology*, 17:1–11, 2021.
- 331 [2] Jessica L McCarty, Christopher O Justice, and Stefania Korontzi. Agricultural burning in the
332 southeastern united states detected by modis. *Remote Sensing of Environment*, 108(2):151–162,
333 2007.
- 334 [3] N Andela, JW Kaiser, GR Van der Werf, and MJ Wooster. New fire diurnal cycle characteriza-
335 tions to improve fire radiative energy assessments made from modis observations. *Atmospheric
336 Chemistry and Physics*, 15(15):8831–8846, 2015.
- 337 [4] Mingxing Tan and Quoc Le. Efficientnetv2: Smaller models and faster training. In *International
338 conference on machine learning*, pages 10096–10106. PMLR, 2021.
- 339 [5] Xinyu Liu, Houwen Peng, Ningxin Zheng, Yuqing Yang, Han Hu, and Yixuan Yuan. Efficientvit:
340 Memory efficient vision transformer with cascaded group attention. In *Proceedings of the
341 IEEE/CVF conference on computer vision and pattern recognition*, pages 14420–14430, 2023.
- 342 [6] Alexey Dosovitskiy, Lucas Beyer, Alexander Kolesnikov, Dirk Weissenborn, Xiaohua Zhai,
343 Thomas Unterthiner, Mostafa Dehghani, Matthias Minderer, Georg Heigold, Sylvain Gelly, et al.
344 An image is worth 16x16 words: Transformers for image recognition at scale. *arXiv preprint
345 arXiv:2010.11929*, 2020.
- 346 [7] Hengshuang Zhao, Jianping Shi, Xiaojuan Qi, Xiaogang Wang, and Jiaya Jia. Pyramid scene
347 parsing network. In *Proceedings of the IEEE conference on computer vision and pattern
348 recognition*, pages 2881–2890, 2017.
- 349 [8] Liang-Chieh Chen, George Papandreou, Iasonas Kokkinos, Kevin Murphy, and Alan L Yuille.
350 Deeplab: Semantic image segmentation with deep convolutional nets, atrous convolution, and
351 fully connected crfs. *IEEE transactions on pattern analysis and machine intelligence*, 40(4):
352 834–848, 2017.
- 353 [9] Enze Xie, Wenhui Wang, Zhiding Yu, Anima Anandkumar, Jose M Alvarez, and Ping Luo.
354 Segformer: Simple and efficient design for semantic segmentation with transformers. *Advances
355 in neural information processing systems*, 34:12077–12090, 2021.
- 356 [10] Tete Xiao, Yingcheng Liu, Bolei Zhou, Yuning Jiang, and Jian Sun. Unified perceptual parsing
357 for scene understanding. In *Proceedings of the European conference on computer vision
(ECCV)*, pages 418–434, 2018.
- 359 [11] René Ranftl, Alexey Bochkovskiy, and Vladlen Koltun. Vision transformers for dense prediction.
360 In *Proceedings of the IEEE/CVF international conference on computer vision*, pages 12179–
361 12188, 2021.